Short-Time Dynamics of Vibrational Relaxation in Molecular Fluids

Branka M. Ladanyi*

Department of Chemistry, Colorado State University, Fort Collins, Colorado 80523

Richard M. Stratt*

Department of Chemistry, Brown University, Providence, Rhode Island 02912

Received: August 1, 1997; In Final Form: October 24, 1997[⊗]

Modern approaches to vibrational relaxation in liquids have begun to move beyond the simple question of how fast vibrational population relaxation occurs to the more challenging question of how it occurs at all: the precise molecular mechanisms by which a solvent stimulates the loss of a vibrational quantum from a solute. We report here some progress in understanding these mechanisms based on looking at the dynamics of the initial triggering events in the vibrational relaxation seen in molecular fluids. With the aid of instantaneous-normal-mode analysis we find a remarkable similarity between vibrational relaxation and the dynamics of solvation. The key concept, in both cases, is that the polarity and general behavior of the solvent is far less important in determining the relevant mechanism than is the particular force or potential monitored by the relevant experiment ("the spectroscopic probe potential"). Vibrational population relaxation automatically accesses the force on a bond, a quantity sufficiently similar to the Lennard-Jones part of the solute−solvent potential that solvation probed by Lennard-Jones potentials ends up sensing a virtually identical mechanism, regardless of the specifics of the liquids. We find that, in both cases, the events that trigger the relaxation typically involve no more than a solvent molecule or two, independently of whether the system is a dipolar solute dissolved in CH_3CN or I_2 dissolved in either liquid or supercritical CO_2. The similarity even extends to the precise spectra of active instantaneous normal modes of the liquid that govern the dynamics for the two very different processes (the "influence spectra"). With a much longer ranged probe potential, such as that found in dipolar solvation, the shape of the influence spectrum does become noticeably different, but even for electrostatics-dominated examples we never find that more than four or five solvents are needed to make up the bulk of the influence spectrum derived from any one liquid configuration. The collective character of solute relaxation evidently does not come into play until times significantly longer than the duration of the triggering events.

I. Introduction

That even the most straightforward of vibrational spectroscopies in liquids has the potential to reveal the intimate details of vibrational dynamics has long been appreciated. The broadening of what would otherwise be a sharp line carries information about all of the static and dynamical features of the vibration's interaction with the surrounding liquid.[1] Separating out those individual features, however, requires more sophisticated experimental probes. Techniques such as infrared[2,3] and Raman echoes[4,5] are now being used to measure how much of the broadening of the absorption arises from solvent motion occurring on time scales comparable to that of the vibration (homogeneous broadening), how much can be thought of as arising from the liquid features that change so slowly they look essentially static (inhomogeneous broadening), and how much falls in between these extremes. Within the realm of homogeneous broadening, there is then the further issue of whether the broadening can be attributed to the finite lifetime of a vibrational excitation (T_1), to the finite lifetime of vibrational phase information within a given vibrational state (T_2*), or to both.[6] Here too, information is rapidly becoming available. Pump−probe measurements of the populations of specific vibrational energy levels yield T_1 values directly,[7−12] from which one can deduce $1/T_2$*, the pure dephasing rate, just by taking the difference between the total dephasing rate associated with the homogeneous line width, $1/T_2$, and the rate arising from vibrational energy relaxation, $1/(2T_1)$.[13]

Having reached this juncture, however, it is important to remember that the point of the whole analysis was not to rationalize the broadening of infrared or Raman lines; it was to understand the vibrations themselves. What one would really like to know are the molecular *mechanisms* by which liquids influence intramolecular dynamics. Simply knowing average lifetimes, for example, constrains the possibilities, but it does not tell us which kinds of motions by the solvent molecules are most efficient in removing vibrational energy. Similarly, just knowing that inhomogeneous broadening contributes a certain fraction of the broadening is informative, but it does not do much to address the question of how the most important solvent dynamics can differ from liquid configuration to liquid configuration.

This notion of mechanism is one that has begun to receive a certain amount of attention from both experiment and theory. In a certain sense, the experiments[11,14,15] and theoretical studies[16] that have traced the flow of vibrational energy from mode to mode within molecules (and between molecules) have provided

[⊗] Abstract published in *Advance ACS Abstracts,* December 15, 1997.

S1089-5639(97)02517-6 CCC: $15.00
Published on Web 01/22/1998

us with the first glimpses of mechanistic detail. More specific information has also begun to become available from simulations that test such matters as the relative efficiencies of electrostatic and nonelectrostatic forces in promoting vibrational relaxation.[17] However there is another, more targeted, theoretical route to such mechanistic information, one that seems particularly well adapted to ferreting out the microscopic origins of at least vibrational population relaxation, that of instantaneous-normal-mode analysis.[18,19] It is this type of approach we wish to pursue in this paper.

The idea behind this perspective is that for any instantaneous configuration of a liquid, the potential surface immediately surrounding the configuration is nearly harmonic, meaning that it is sensible to imagine any motion taking place starting from that configuration as being decomposable into (instantaneous) harmonic modes. These modes (INMs) will change from configuration to configuration, but at any instant they provide a natural set of well-defined collective solvent motions; indeed for short enough times, they provide *the* natural set of motions. One can therefore analyze even relatively complicated aspects of the short-time solvent dynamics by resolving the motion into linear combinations of INMs.[20−27] Moreover, because one knows the specific molecular ingredients of each mode, it then becomes possible to compute the average fraction of the important dynamics governed by any proposed model of the motion: that stemming from longitudinal, rather than transverse, motion, say, or from nearby, rather than distant, solvents. Just such a program has been carried out in the course of investigating the dynamics of solvation[22,23] and, in a more preliminary fashion, for vibrational relaxation.[24,26]

Beyond presenting this kind of averaged information, however, an instantaneous perspective obviously allows us to look directly at the specific dynamics associated with specific liquid configurations. Both solvation dynamics and vibrational relaxation have begun to be subjected to this, deeper, more revealing, level of analysis.[28] In the results to date, which have been limited to studying the effects of relatively short-ranged forces and to atomic solvents, almost all of the relaxation dynamics affiliated with a given liquid configuration was found to be attributable to the influence of the key INMs on one or two critical solvent atoms, a finding strikingly reminiscent of the venerable binary collision theory of vibrational relaxation.[29,30] Perhaps as a direct result of this few-body dominance, the average spectra of contributing modes in solvation and in vibrational relaxation examples have been found to be strikingly similar to each other in atomic fluids.[28] Still unknown, though, is the extent to which these observations will survive the generalization to molecular solvents and to a wider range of intermolecular interactions.

What we shall be concerned with in this paper is the application of our linear instantaneous-normal-mode approach to vibrational population relaxation under these more general circumstances. In our previous work, we demonstrated that an INM treatment of an atomic solvent, in combination with the assumption that displacement of the solute vibration in question is linearly coupled (coupled at the one-phonon level) to the solvent, suffices to yield an instantaneous generalized Langevin equation for the vibrating coordinate.[25] This result, in turn, provides us with the instantaneous friction the coordinate sees, from which the desired relaxation dynamics follows easily. The intrinsic limitations of the INM formalism preclude us from examining the zero-frequency friction that we need to predict $1/T_2^*$, the pure dephasing rate,[31] but $1/T_1$, the vibrational population relaxation rate, can be computed at the Landau−Teller level just by evaluating the cosine transform of the INM friction at the frequency of the vibration.[6,7,17,32,33]

In this paper we shall apply this formalism to vibrations of diatomic molecules dissolved in two different molecular fluids, one nondipolar, carbon dioxide, and the other manifestly polar, acetonitrile. With molecular solvents we can certainly ask about such explicitly molecular issues as the relative importance of solvent center-of-mass translation and solvent libration, but more importantly with these examples we can contrast the instantaneous dynamics of short-ranged repulsive interactions with that generated when dispersion and electrostatic forces come into play. We shall ascertain, in particular, what happens to the few-body character of the instantaneous relaxation channels as the range of interaction increases, and we shall ask how universal the similarity is between solvation and vibrational relaxation.

The remainder of the paper is organized as follows: In section II we review the linear INM formalism used in studying vibrational and solvation relaxation, focusing on what we call the influence spectra for these processes. We also review how mechanistic information can be extracted from the exact time evolution as revealed by molecular dynamics. In section III, we summarize our calculational procedures and models, and in section IV, we present our results, both for instantaneous and averaged relaxation dynamics. We conclude in section V with some general comments.

II. Formalism

A. Linear Instantaneous-Normal-Mode Treatments of Vibrational Relaxation and Solvation Dynamics. Our basic approach for treating liquid-state spectroscopy problems within linearly coupled INM theory was first elaborated several years ago.[21] The formalism has since been applied to solvation dynamics,[22,23] to vibrational relaxation,[24−26] and to infrared, Raman, and optical Kerr effect spectroscopies,[27] as well as to some of the more general features of solute relaxation common to the first two processes.[28] During the course of these applications we have had occasion to discuss in some depth the assumptions, limitations, and levels of quantitative success characteristic of this approach. We will therefore confine ourselves here to recounting only enough of the results to be able to define the crucial quantities.

The focus of the theory is the weighted spectrum of the INM frequencies of the solution, what we have termed the *influence spectrum* for the process being considered. For any given liquid configuration **R**, the spectrum is defined to be

$$\rho_{\mathbf{R}}(\omega) = \sum_{\alpha} c_{\alpha}{}^{2}\delta(\omega - \omega_{\alpha}) \tag{2.1}$$

where the sum is over all the instantaneous normal modes of the given configuration α, the ω_α are the frequencies of the modes, and the coefficients c_α represent the efficiency with which each mode affects the microscopic dynamics behind the spectroscopic observable. In particular, for pump−probe measurements of vibrational population lifetimes (with the observable being the populations of the vibrational states), the microscopically interesting function ends up being the force along the vibrating bond.[25] For time-dependent fluorescence studies of solvation dynamics,[34] the observable is the time evolution of the emission frequency, making the relevant microscopic quantity the difference in the solute−solvent interaction energy between ground- and electronically-excited-state solute.[22,23] More generally, if the microscopically pertinent quantity is some function of the solute and solvent nuclear

coordinates, A, then the coupling constant for the αth mode is

$$c_\alpha = \partial A/\partial q_\alpha \tag{2.2}$$

with q_α the (mass-weighted) instantaneous-normal mode coordinate for mode α.

These influence spectra are actually quite revealing in themselves, but the simplest direct connections with spectroscopy are through time correlation functions involving the A's, which we can calculate from the *averaged* influence spectra,

$$\rho_A(\omega) = \langle \rho_{\mathbf{R}}(\omega) \rangle \tag{2.3}$$

where the average is over the liquid configurations **R**. The spectroscopic "velocity" autocorrelation functions,

$$G_{AA}(t) = \langle \dot{A}(0)\dot{A}(t) \rangle = -\frac{\mathrm{d}^2}{\mathrm{d}t^2}\langle A(0)A(t) \rangle \tag{2.4}$$

are particularly straightforward to obtain, inasmuch as they are predicted to be simply the time-domain version of the averaged influence spectra,[21]

$$G_{AA}(t) = (k_\mathrm{B}T)\int \mathrm{d}\omega\ \rho_A(\omega)\cos(\omega t) \tag{2.5}$$

For solvation dynamics, for example, these last equations mean that we can compute the experimentally accessible energy-gap correlation function itself just by taking a double-time integral of the relevant $G(t)$ function.[22,23,30]

For vibrational relaxation, we find the second derivative of the vibrational friction $\eta(t)$ to be given by a similar expression:[24,25]

$$\frac{\mathrm{d}^2}{\mathrm{d}t^2}\eta(t) = -\int \mathrm{d}\omega\ \rho_{\mathrm{vib}}(\omega)\cos(\omega t) \tag{2.6}$$

Thus, if the interest is then in the T_1 lifetime of a vibrating diatomic with (solution-phase) frequency ω_0 and reduced mass μ, because we know that the cosine transform of this friction determines T_1,

$$1/T_1 = \mu^{-1}\eta_\mathrm{R}(\omega_0) \tag{2.7}$$

$$\eta_\mathrm{R}(\omega_0) = \int_0^\infty \mathrm{d}t \cos(\omega t)\ \eta(t) \tag{2.8}$$

within Landau−Teller theory,[6,7,17,32] we can see from eq 2.6 that we should expect the desired relaxation rate to be proportional to the averaged influence spectrum itself:[35]

$$\eta_\mathrm{R}(\omega) = (\pi/2)\omega^{-2}\rho_{\mathrm{vib}}(\omega) \tag{2.9}$$

All of these results depend, of course, on being able to calculate the instantaneous normal modes of the solutions we wish to study. These modes are obtained in this paper, as has become standard, by using simulation to generate an equilibrium distribution of liquid configurations and then constructing the dynamical matrix—the mass-weighted Hessian matrix of second derivatives of the potential energy—for each of the resulting configurations. With the rigid linear models of the solvents and solutes we consider in this paper, these matrices end up being $5(N+1) \times 5(N+1)$, corresponding to the three center-of-mass translations and the two spherical-polar orientational angles associated with the single solute molecule and with each of the N solvent molecules. The eigenvalues and eigenvectors of the dynamical matrices then yield the necessary INM frequencies and modes, respectively. Further details may be found in refs 22 and 36.

B. Mechanistic Analysis. As noted by Steele,[37] the velocity form of time correlation functions proves to be a useful quantity to contemplate even when we are not interested in INM approaches. It is always possible to write time derivatives of the dynamical variable of interest rigorously as a sum over contributions from each coordinate of each molecule

$$\dot{A}(t) = \sum_{j\mu}(\partial A/\partial r_j)_t\ \dot{r}_{j\mu}(t) \tag{2.10}$$

where $j = 0, ..., N$ labels the solute and the N solvent molecules (respectively), the subscript t indicates that the derivative is to be evaluated with all of the coordinates at their time t values, and the molecular coordinates are taken to be $\mu = x, y, z, \theta, \phi$ for our systems. The full $G_{AA}(t)$ correlation function of eq 2.4 involves all of the terms in this sum for $\dot{A}(t)$, as well as all of the terms for $\dot{A}(0)$, but one could imagine separating out any subset of these coordinates for closer examination. For example, we could partition $G_{AA}(t)$ into rotational and translational components by looking at

$$\dot{A}^{\mathrm{rot}}(t) = \sum_j \sum_{\mu=\theta,\phi} (\partial A/\partial r_{j\mu})_t\ \dot{r}_{j\mu}(t)$$

$$\dot{A}^{\mathrm{trans}}(t) = \sum_j \sum_{\mu=x,y,z} (\partial A/\partial r_{j\mu})_t\ \dot{r}_{j\mu}(t)$$

Since $\dot{A}(t) = \dot{A}^{\mathrm{rot}}(t) + \dot{A}^{\mathrm{trans}}(t)$, we can write

$$G_{AA}(t) = G_{AA}^{\mathrm{rot}}(t) + G_{AA}^{\mathrm{trans}}(t) + G_{AA}^{\mathrm{cross}}(t) \tag{2.11}$$

where the purely rotational, purely translational, and cross contributions are

$$G_{AA}^{\mathrm{rot}}(t) = G_{\dot{A}^{\mathrm{rot}}\dot{A}^{\mathrm{rot}}}(t), \quad G_{AA}^{\mathrm{trans}}(t) = G_{\dot{A}^{\mathrm{trans}}\dot{A}^{\mathrm{trans}}}(t)$$

$$G_{AA}^{\mathrm{cross}}(t) = G_{\dot{A}^{\mathrm{rot}}\dot{A}^{\mathrm{trans}}}(t) + G_{\dot{A}^{\mathrm{trans}}\dot{A}^{\mathrm{rot}}}(t)$$

An interesting, but slightly different, partitioning lets us think about the distinction between the *binary* dynamics (b) induced by the motion of the solute and a single solvent molecule at a time, and the remaining dynamics, which is intrinsically *ternary* (t) since it can be thought of as stemming from the simultaneous motion of the solute and two different solvents. If, as in our case, the spectroscopic probe function A can be written as a sum of pair potentials acting between the solute 0 and each of the solvent molecules j,

$$A = \sum_{j=1}^{N} w_{0j}, \quad w_{0j} = w(\mathbf{r}_{0j}, \hat{\Omega}_0, \hat{\Omega}_j) \tag{2.12}$$

with $\hat{\Omega}_j$ the orientational unit vector of molecule j prescribed by (θ_j,ϕ_j), then its time derivative neatly separates into a sum of terms associated with the motion of each solvent molecule in concert with the solute.

$$\dot{A}(t) = \sum_{j=1}^{N} \Delta\dot{A}_j(t)$$

$$\Delta A_j(t) = \sum_\mu [(\partial w_{0j}/\partial r_{j\mu})_t\ \dot{r}_{j\mu}(t) + (\partial w_{0j}/\partial r_{0\mu})_t\ \dot{r}_{j\mu}(t)] \tag{2.13}$$

The velocity form of the correlation function can therefore be dissected into the desired binary and ternary pieces:

$$G(t) = G^b(t) + G^t(t)$$

$$G^b(t) = \sum_{j=1}^{N} \langle \Delta\dot{A}_j(0)\, \Delta\dot{A}_j(t) \rangle$$

$$G^t(t) = \sum_{\substack{j,k=1 \\ (j\neq k)}}^{N} \langle \Delta\dot{A}_j(0)\, \Delta\dot{A}_k(t) \rangle \qquad (2.14)$$

The ordinary (nonvelocity version of the) time correlation function $\langle A(0)\, A(t) \rangle$ can, of course, also be divided into one- and two-solvent portions, but it is worth emphasizing that such an approach may not serve to partition the correlation function into contributions from different *motions*, that is, into different velocities, $dr_{j\mu}/dt$. Indeed, at short times the apparent distinction between these binary and ternary terms reflects little more than the existence of separate binary and ternary contributions to the zero time value,

$$\langle A(0)\, A(0) \rangle = \sum_{j=1}^{N} \langle w_{0j}(0)\, w_{0j}(0) \rangle + \sum_{\substack{j,k=1 \\ (j\neq k)}}^{N} \langle w_{0j}(0)\, w_{0k}(0) \rangle$$

a separation which arises as a consequence of the equilibrium liquid structure and has no direct implications for the dynamical mechanism.

The usefulness of a velocity-based analysis is emphasized even more in linear INM treatments, which effectively replace the generalized forces $(\partial A/\partial r_{j\mu})_t$ evaluated along the exact trajectory, $\mathbf{R}(t)$, with their instantaneous ($t = 0$) counterparts.[21] In this approximation—which is exact at short enough times—all of the dynamics resides in the $\dot{r}_{j\mu}(t)$'s, meaning that all of the mechanistic analysis that we carry out revolves around these velocities. The outcomes of these kinds of INM investigations have usually been reported in the frequency domain as projections of the averaged INM influence spectra, eqs 2.1 and 2.3, but the ideas are basically the same as what we have been discussing. For discriminating between rotational and translational contributions, for example,[22,23] we have shown that the influence spectra should be partitioned as

$$\rho_A(\omega) = \rho_A^{\mathrm{rot}}(\omega) + \rho_A^{\mathrm{trans}}(\omega) + \rho_A^{\mathrm{cross}}(\omega)$$

$$\rho_A^{\mathrm{rot}}(\omega) = \langle \sum_{\alpha} (c_\alpha^{\mathrm{rot}})^2 \delta(\omega - \omega_\alpha) \rangle$$

$$\rho_A^{\mathrm{trans}}(\omega) = \langle \sum_{\alpha} (c_\alpha^{\mathrm{trans}})^2 \delta(\omega - \omega_\alpha) \rangle$$

$$\rho_A^{\mathrm{cross}}(\omega) = \langle 2 \sum_{\alpha} (c_\alpha^{\mathrm{rot}})^2 (c_\alpha^{\mathrm{trans}}) \delta(\omega - \omega_\alpha) \rangle \qquad (2.15)$$

with the projected coefficients (defined from eq 2.2)

$$c_\alpha^{\mathrm{rot}} = \sum_j \sum_{\mu=\theta,\phi} (\partial A/\partial r_{j\mu})_0\, (\partial r_{j\mu}/\partial q_\alpha)$$

$$c_\alpha^{\mathrm{trans}} = \sum_j \sum_{\mu=x,y,z} (\partial A/\partial r_{j\mu})_0\, (\partial r_{j\mu}/\partial q_\alpha) \qquad (2.16)$$

bringing in the instantaneous generalized forces and the INM eigenvectors. From eq 2.5, then, the INM time-domain equivalents are

$$G_{AA}^{\mathrm{rot}}(t) = (k_{\mathrm{B}}T) \int \mathrm{d}\omega\, \rho_A^{\mathrm{rot}}(\omega) \cos(\omega t) \qquad (2.17)$$

and similarly for the translational and cross-correlation functions. Thus, with the aid of such projections we can use INM theory to get at either frequency- or time-domain pictures of the mechanisms of solute relaxation.

III. Models and Computational Details

We present here the results for two model dilute solutions, one representing I_2 dissolved in CO_2 and the other mimicking a dipolar diatom with bromine-like Lennard-Jones (LJ) potential parameters and a bromine-like bond length dissolved in acetonitrile. For simulation purposes, the solute and solvent molecules are always assumed to be rigid, with bond lengths and angles fixed at their isolated-molecule equilibrium values. The intermolecular potentials that we use are sums of LJ + Coulomb site−site terms. For a pair of sites a and b on different molecules they are given by

$$u_{ab}(r) = 4(\epsilon_a\epsilon_b)^{1/2}\left\{\left(\frac{\sigma_a+\sigma_b}{2r}\right)^{12} - \left(\frac{\sigma_a+\sigma_b}{2r}\right)^{6}\right\} + \frac{Q_aQ_b}{4\pi\epsilon_0 r} \qquad (3.1)$$

where ϵ_a and σ_a are the LJ well depth and diameter of site a and Q_a is its partial charge. As eq 3.1 indicates, Lorentz−Berthelot combining rules[38] are used to determine the LJ potential parameters for pairs of unlike sites. For acetonitrile, we use the Edwards et al.[39] potential in which the methyl group is a single interaction site, making the molecule effectively linear. For CO_2, we use the five-site potential we developed,[23] based on the LJ parameters given by Murthy et al.[40] and on five partial charges chosen to give the three lowest permanent moments determined by Stone and Alderton.[41] The solute LJ potential parameters are taken from Rappé el al.[42] For I_2, the three partial charges were chosen to give the calculated value (5.57 D Å)[43] of the molecular quadrupole. The dipolar "Br_2" is constructed with two partial charges, giving it a dipole moment of 5.47 D. The potential parameters and molecular geometries for the dipolar "Br_2"−acetonitrile system are summarized in Table 1 of ref 22, and those for the I_2−CO_2 system are reported in Table 2 of ref 23.

In the case of the I_2−CO_2 system, we simulated three thermodynamic states, one at 220 K and 1.128 g/cm^3, corresponding to the liquid near its triple point,[44,45] and two others in the supercritical fluid state.[46] Both of these supercritical simulations were carried out at 320 K, but one of them was at the critical density ρ_c of 0.467 g/cm^3 and the other at 2.5 times this density. The dipolar "Br_2"−CH_3CN system was simulated at conditions corresponding to the liquid at room temperature and atmospheric pressure, 293 K and 0.7867 g/cm^3. As in our previous work,[22,23] the molecular dynamics (MD) simulations were carried out in the microcanonical ensemble, and Ewald sums with conducting boundary conditions were employed for Coulombic interactions.[38] In the case of the I_2−CO_2 system, the equations of motion were integrated using time steps of 6 fs for the liquid state and 5 fs for the supercritical states. Time steps of 8 fs were used for the dipolar "Br_2"−CH_3CN system. Further details of the simulation technique and of the subsequent calculation of the INM eigenvectors and eigenvalues can be found in ref 22.

All the INM results that we present were obtained for systems containing one solute and 107 solvent molecules. To ascertain

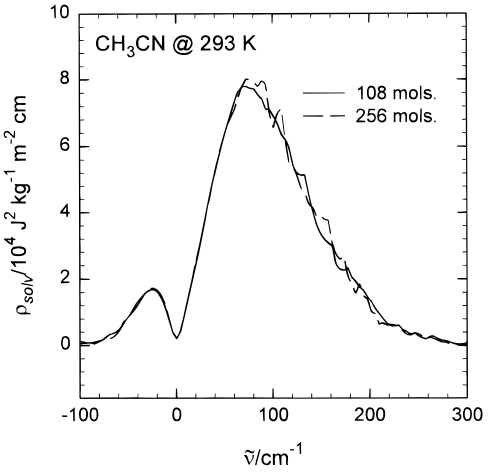

Figure 1. Solvation for a dipolar-diatomic solute dissolved in liquid CH_3CN illustrating the extent of finite-size effects in INM calculations of relaxation in polar solvents. The labels on the two curves indicate the number of molecules involved in both simulations (including the one solute in each case). The differing amounts of noise reflect that the fact that the curve for the smaller simulation represents an average over four times as many liquid configurations as the curve for the larger simulation.

that systems of this size are sufficiently large to give results representative of macroscopic solution samples, we also carried out MD simulations of one solute−255 solvent systems. Comparison of $\eta(t)$, $G_{\text{vib}}(t)$, and $G_{\text{solv}}(t)$ obtained from MD trajectory data for 108- and 256-molecule systems showed no significant system size effects, even in the case with the longest range interactions, dipolar "Br_2"−CH_3CN. For this system we have also studied the system size dependence of the INM influence spectra for electrostatic solvation. The results are shown in Figure 1. The small differences that are seen between the two sets of $\rho_{\text{solv}}(\omega)$ data are due to the higher noise level in the spectrum for the 256-molecule system, which corresponds to an average over 200 liquid configurations, while the 108-molecule system data correspond to an average over 800 configurations. All the other influence spectra that we calculate correspond to shorter ranged functions of solute−solvent distances and should therefore show even weaker system size dependence.

The INM influence spectra for the dipolar "Br_2"−CH_3CN system were obtained by averaging over 800 configurations separated by 0.8 ps. For the I_2−CO_2 system in liquid state we used 1000 configurations separated by 0.6 ps, and for this system at 320 K the influence spectra correspond to averages over 1200 configurations separated by 0.5 ps.

In addition to these INM predictions for friction spectra, the MD-calculated $\eta(t)$ was also used to compute the frequency-domain vibrational friction $\eta_R(\omega)$. The necessary transform was evaluated by fitting the simulated data to a simple functional form and then transforming the fit, as detailed in the Appendix.

IV. Results

A. Basic Features of Vibrational Friction in Molecular Fluids. The first observation that one makes when confronting the results on vibrational relaxation for specifically molecular solvents is that, at least for frequencies under a few hundred cm^{-1}, molecular and atomic solvents are not all that dissimilar in their abilities to absorb excess vibrational energy from a solute.[24,26,47] As we can see from our results for the frequency-dependent vibrational friction in Figure 2, neither the addition of orientational degrees of freedom nor the new-found distinctions between nonpolar and dipolar solvents seem to change the qualitative behavior of the friction. Both liquid CO_2 and liquid CH_3CN, for example, have a sharp downturn at very low frequencies followed by a more gradual decay at higher frequencies. Indeed, the fact that there are *quantitative* similaries between vibrational population relaxation rates in these two superficially very different liquids is strikingly reminiscent of the close parallels between the ultrafast solvation processes in these same systems.[23]

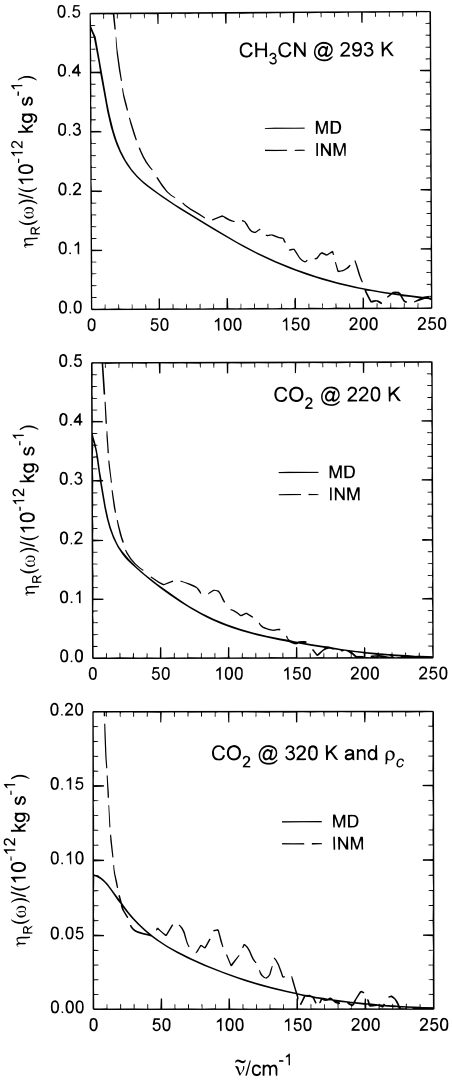

Figure 2. Frequency dependence of vibrational friction felt by a diatomic solute. Shown here are comparisons of the real part of the frequency-domain friction computed by molecular dynamics (MD) (from the Fourier transform of the fluctuations in force on the rigid bond) with that computed from instantaneous-normal-mode theory (INM). Starting at the top, the three panels correspond to a dipolar solute dissolved in liquid CH_3CN, I_2 dissolved in liquid CO_2, and I_2 dissolved in supercritical CO_2 at the critical density.

For our purposes here, the other noteworthy feature of these plots is the extent to which the INM predictions tend to match the molecular dynamics results. Though they are not as accurate in the supercritical regime as they are in dense liquids, the instantaneous-normal-mode results seem to be remarkably good at capturing the overall scale and essential features of the friction. They even succeed in predicting the roughly factor-of-2 dimunition of the friction that one sees on going from dense liquid to supercritical CO_2. Of course, the limitations of this level of theory should also be kept in mind. The inability of this level of theory to cope with diffusion means that our INM

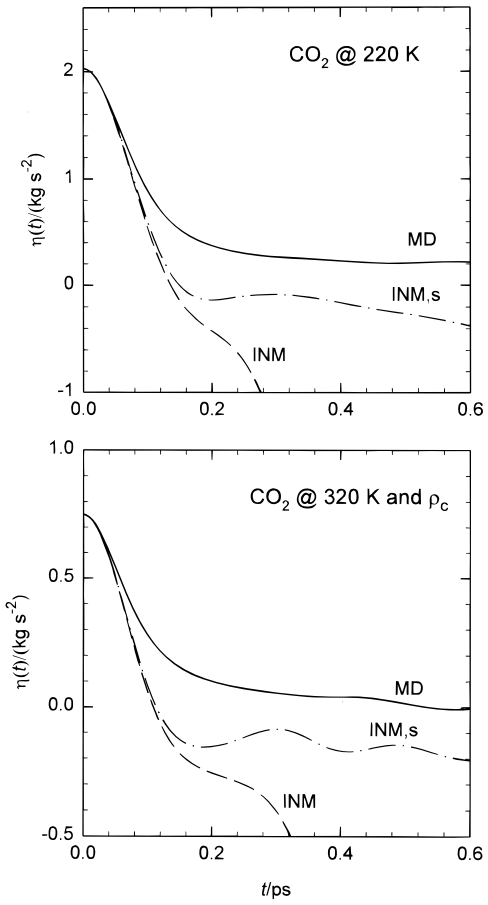

Figure 3. Time dependence of vibrational friction felt by a diatomic solute. Molecular dynamics (MD) calculations are compared with those of instantaneous-normal-mode (INM) theory, as in Figure 2, with the INM and INMs curves corresponding to the results with and without the inclusion of imaginary modes (respectively). The top and bottom panels display the comparisons for I_2 dissolved in liquid CO_2 and for I_2 dissolved in supercritical CO_2 at the critical density.

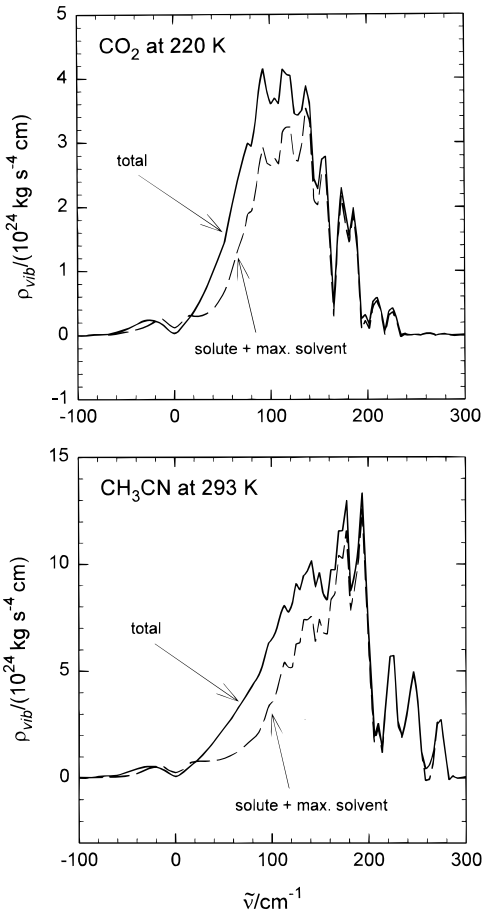

Figure 4. Vibrational friction influence spectra for I_2 dissolved in liquid CO_2 and for a dipolar solute dissolved in liquid CH_3CN. Each panel compares the full influence spectrum with the corresponding projected spectrum in which only the motion of the solute and the single most strongly coupled solvent are included.

friction is compelled to diverge at the very lowest frequencies instead of simply exhibiting a maximum (and, in the supercritical fluid case, not all that pronounced a maximum) at zero frequency.[26] Perhaps less obvious from the figure is that the highest frequency behavior has difficulties as well. INM spectra will always be essentially zero for frequencies outside the few hundred cm^{-1} range allowed for the INM bands in these liquids. The true molecular dynamics, in contrast, should predict the existence of the tiny but finite relaxation rates that one sees experimentally for modes some 10 times higher in frequency.[7,48]

This low-frequency irregularity is highlighted in the time-domain version of these vibrational friction results, Figure 3. The rapid Gaussian-like falloff of the friction in the first 200 fs seems to be treated adequately, if not quantitatively, by INM theory, at least for dense liquids. However the longer time behavior is qualitatively incorrect; the INM curves slowly (logarithmically) decay to $-\infty$ instead of to 0, leading to significant disparities by 0.5 ps. Clearly, it is well to remember that INM theory is designed to work only at short times.[25] Fortunately, most of the dynamics we wish to investigate in this paper is governed by that first 200 fs, so we shall concentrate our efforts there.

So what kinds of insights can one garner from an INM analysis of vibrational relaxation in these fluids? The influence spectrum for vibrational relaxation, eqs 2.1 and 2.3, hold a variety of clues as to the underlying mechanisms. Consider, for example, the question of which molecules act as the principal agents of vibrational relaxation. Our previous studies in atomic fluids led to the interesting but maybe not all that surprising result that the vibrational population relaxation that one sees at any one instant of time is largely triggered by one or two active solvents.[26,28] We might be able to understand such extreme localization given the incredibly short range of the repulsive force between atoms. But what should happen in a molecular fluid with its much more complicated packing geometries and, a fortiori, in a polar fluid, where much longer ranged forces operate?[49] From Figure 4, we see that there is little, if any, mechanistic difference between molecular and atomic fluids at this level. The INM formalism allows us to project out the contributions of the single solvent molecule which most effectively modulates the coupling to the vibrating diatomic (Table 1).[50] When the contributions of this "maximum" solvent are added to those of the solute itself,[51] we find that we can account for more than three-fourths of the total influence spectrum with just this binary motion: 76% for liquid CO_2 and 77% for the (dipolar) liquid CH_3CN. Moreover with liquid CO_2, 84% of this binary part (a total of 64%) arises specifically from the solute and the solvent nearest the solute (in a site−site distance sense),[52] a result strikingly similar to the total of 65% seen in the atomic solvent case.

With the atomic fluid, the observation of this strongly binary character for the instantaneous relaxation prompted us to ask whether we were really validating the isolated-binary-collision (IBC) theory for vibrational relaxation.[29,53,54] It is easy enough to look, as we did in the earlier work,[26] at whether the vibrational

TABLE 1: Effects of Different Solvents on the Dynamics of Vibrational Relaxation[a]

system	translational dynamics[b] (%)	binary dynamics[c] (%)
liquid CO_2[d]	62.6	75.8
supercritical CO_2 (ρ_c)[e]	61.1	90.8
supercritical CO_2 ($2.5\rho_c$)[e]	61.9	76.6
liquid CH_3CN[f]	60.1	76.8

[a] Fraction of the prompt vibrational relaxation dynamics arising from the particular kind of motion (as measured by the percentage of the influence spectrum associated with the indicated type of dynamics). [b] Percentage of the influence spectrum arising from center-of-mass translation of the solute and the solvent molecules. [c] Percentage of the influence spectrum arising from the dynamics of the solute and the single most important solvent molecule. [d] I_2 dissolved in CO_2 at a temperature $T = 220$ K. [e] I_2 dissolved in CO_2 at a temperature $T = 320$ K and at solvent densities equal to and 2.5 times the critical density. [f] Dipolar "Br_2" dissolved in CH_3CN at a temperature $T = 293$ K.

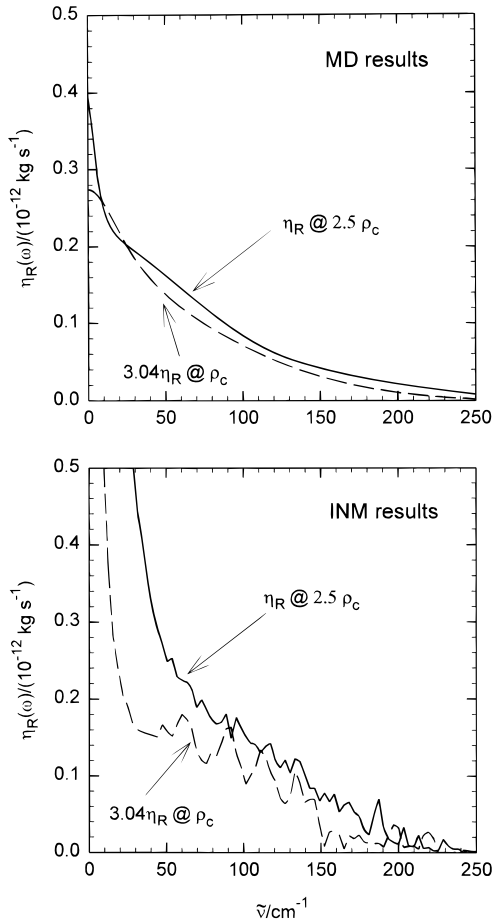

Figure 5. How the vibrational friction for an I_2 solute dissolved in CO_2 at 320 K scales with solvent density. Shown in each panel is a comparison between $\eta_R(\omega)$, the real part of the frequency-domain friction, at 2.5 times the critical density and a scaling factor times the $\eta_R(\omega)$ computed right at the critical density. The scaling factor, 3.04, is the ratio of the local solvent densities at the solute under the two conditions. The two panels display the scaling observed with molecular-dynamics-derived friction and with friction computed from INM theory.

friction we see scales with solvent density in the way that the IBC model would predict. Figure 5 compares the vibrational friction seen in supercritical CO_2 at liquid densities ($\rho = 2.5$ times the critical density ρ_c) with that at the critical density, both at 320 K. The latter friction is noticeably smaller, but if we multiply it by the ratio of local solvent densities in contact with the I_2 solute, $\rho_{loc}(\rho)$, for these two cases, $\rho_{loc}(2.5\rho_c)/\rho_{loc}(\rho_c) = 3.04$, we find that the molecular-dynamics-derived frictions are indeed proportional to the local solvent density, exactly as the IBC theory would have us believe the (hypothetical) collision rates would be.[53] [ρ_{loc} is defined here as $\rho\, g_{IO}(r^*)$, where ρ is the bulk solvent density, $g_{IO}(r)$ is the site−site radial distribution function for distances r between solute I site and solvent O sites, and $r^* = 3.82$ Å is the location of the maximum of the $g_{IO}(r^*)$ when $\rho = 2.5\ \rho_c$ and $T = 320$ K.]

By the same token, though, it is easy to see that there is no need to invoke a gas-phase-like collision in order to explain these results. The bottom panel of Figure 5 illustrates the fact that the INM theory—which postulates that the solvent molecules are moving harmonically in a field of force created by the solvent as a whole—displays much the same density scaling. Even the breakdown of IBC scaling at very low frequencies is successfully mimicked by this harmonic perspective. What we are left with, then, is that at all but the lowest vibrational frequencies solute−solvent pair motions—but not necessarily isolated collisions—are what really stimulates vibrational population relaxation in molecular liquids. Polar liquids, moreover, are no different from nonpolar ones in this reliance on the solvent dynamics in the immediate vicinity of the solute.

B. Relationship between Vibrational Relaxation and Solvation. In the atomic-fluid case we suggested that this crucial role played by binary dynamics is what is fundamentally responsible for some remarkable similarities between vibrational relaxation and solvation.[28] The influence spectra of the two processes, for example, turned out to be virtually identical. How parallel is the situation in molecular fluids? We begin our analysis by reminding ourselves how solvation dynamics itself takes place in molecular solvents.

Solvation studies, unlike vibrational relaxation measurements, allow us to separate two rather different roles played by the intermolecular forces. Clearly the forces present in the solution determine all of the liquid properties which are independent of the particulars of the experiment: the equilibrium intermolecular structure and the instantaneous normal modes of the liquid, for example. They also determine the force along a vibrating bond that governs how that vibrational energy is dissipated. However, solvation experiments such as time-dependent fluorescence[34,55] and transient hole burning[56] actually probe the difference in solute−solvent potentials for two different electronic states of the solute, meaning that an alternative choice of electronic states could in principle access different features of the dynamics of a given liquid. With this possibility in mind, it was natural for our previous solvation studies to try to distinguish the implications of different choices for the spectroscopic probe function, the A we spoke in section II, from the consequences of choosing different kinds of solutions.[23,57]

What we discovered in this earlier work was that the *mechanism* of solvation revealed by experiments in molecular fluids was determined far more by the choice of spectroscopic probe function than by the nature of the solution. Most notably, the extent to which the prompt solvation derives from librational motion (as opposed to relying on center-of-mass translation) depends almost entirely on the symmetry of the probe function. Electrostatic probes in particular (whether dipolar or quadrupolar) are qualitatively different from dispersion and Lennard-Jones probes, more or less independently of whether the solution itself is polar.[23]

With the current study, we can see that vibrational relaxation actually fits nicely into this same pattern. From the comparison of the vibrational friction influence spectrum in liquid CO_2 with that associated with solvation in the same liquid (Figure 6), it is clear that vibrational friction corresponds to an experimental

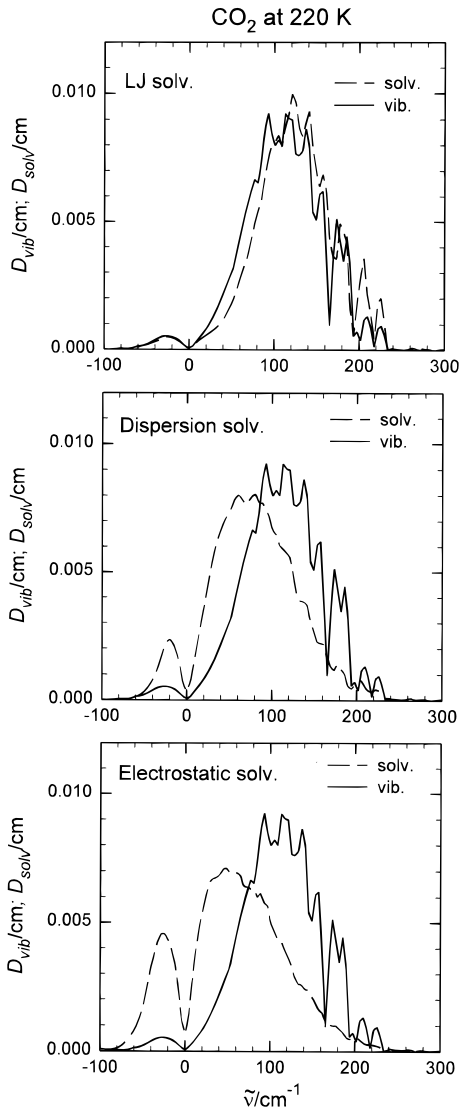

Figure 6. Relationship between vibrational relaxation and solvation dynamics for an I_2 solute dissolved in liquid CO_2. We compare here the normalized influence spectrum for vibrational relaxation (vib.) with the normalized influence spectra for three different choices of solvation (solv.) probe potentials: Lennard-Jones, dispersion, and electrostatic. The normalized spectra $D(\omega) = \rho(\omega)/\int\rho(\omega)\,d\omega$ are employed so as to enable us to make meaningful comparisons between quantities with different units and between quantities with the same units but very different absolute magnitudes.

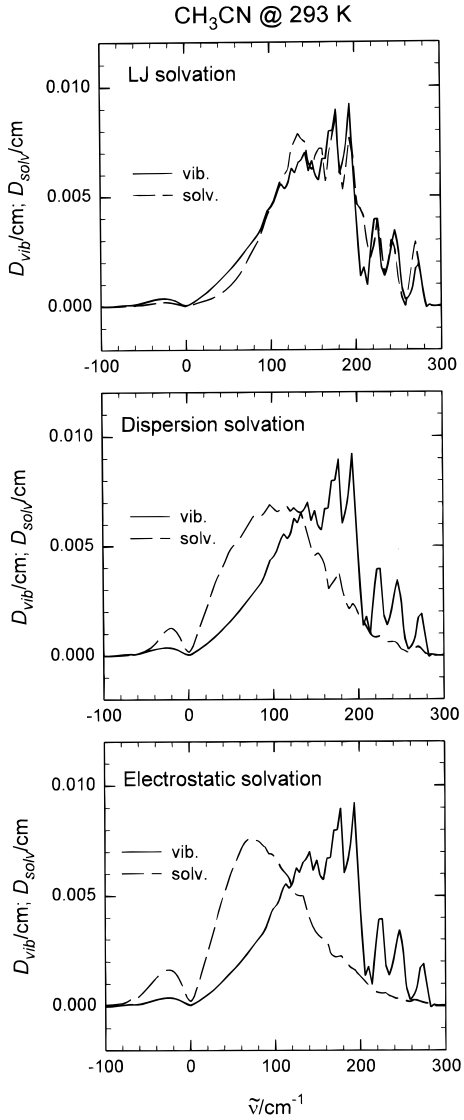

Figure 7. Relationship between vibrational relaxation and solvation dynamics for a dipolar solute dissolved in liquid CH_3CN. We compare here the normalized influence spectrum for vibrational relaxation (vib.) with the influence spectra for three different choices of solvation (solv.) probe potentials: Lennard-Jones, dispersion, and electrostatic.

probe that is evidently in the same "universality class" as Lennard-Jones solvation. The influence spectra for these two processes are remarkably similar, a similarity that becomes progressively less pronounced as one proceeds from a Lennard-Jones solvation probe to a dispersion solvation probe to an electrostatic solvation probe. Moreover, as with Lennard-Jones solvation, we find that the clean separation into predominately librational or translational mechanisms is all but absent with vibrational relaxation. Projection of the vibrational influence spectrum into rotational and translations parts (Table 1) reveals that 62.6% of the prompt dynamics is translational, a figure markedly different from the 80% and 30% seen in the dispersion and electrostatic solvation in liquid CO_2 (respectively), but rather similar to the 55% observed with Lennard-Jones solvation in the same liquid.[23] Much the same behavior is found if we now switch the solvent to the (superficially) very different liquid CH_3CN (Figure 7). Once again, the vibrational friction spectrum ends up lying on top of the Lennard-Jones solvation spectrum, but we see a distinction grow in as the solvation probe is changed from Lennard-Jones to dispersive to electrostatic.

TABLE 2: Role of Binary Dynamics in Solute Relaxation[a]

	vibrational relaxation (%)	solvation[b] (%)		
		LJ	dispersive	electrostatic
liquid CO_2[c]	75.8	71.5	38.1	39.9
liquid CH_3CN[d]	76.8	71.4	38.2	21.5

[a] Percentage of the influence spectrum arising from the dynamics of the solute and the single most important solvent molecule. [b] Solvation dynamics as probed by Lennard-Jones (LJ), dispersion forces (dispersive), or electrostatic interactions (electrostatic). [c] Temperature $T = 220$ K. [d] Temperature $T = 293$ K.

That this pattern of behavior actually results from the binary component of the solution dyamics is now fairly easy to demonstrate. If we project out the fraction of the solvation influence spectrum resulting from the motion of the solute and the single most important solvent, Table 2, we find not only that Lennard-Jones solvation (in both polar and nonpolar solvents) is dominated by binary dynamics to much the same degree as vibrational friction is, but that the percentage of the

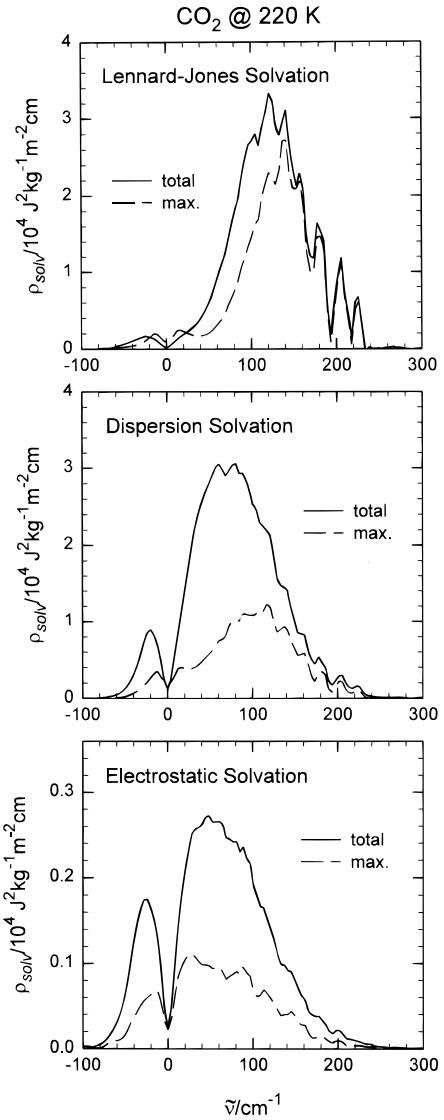

Figure 8. Solvation influence spectra for an I_2 solute dissolved in liquid CO_2. Each panel compares the full influence spectrum (total) with the corresponding projected spectrum in which only the motion of the solute and the single most strongly coupled solvent are included (max.). The three panels reflect three different choices of solvation probe potentials: Lennard-Jones, dispersion, and electrostatic.

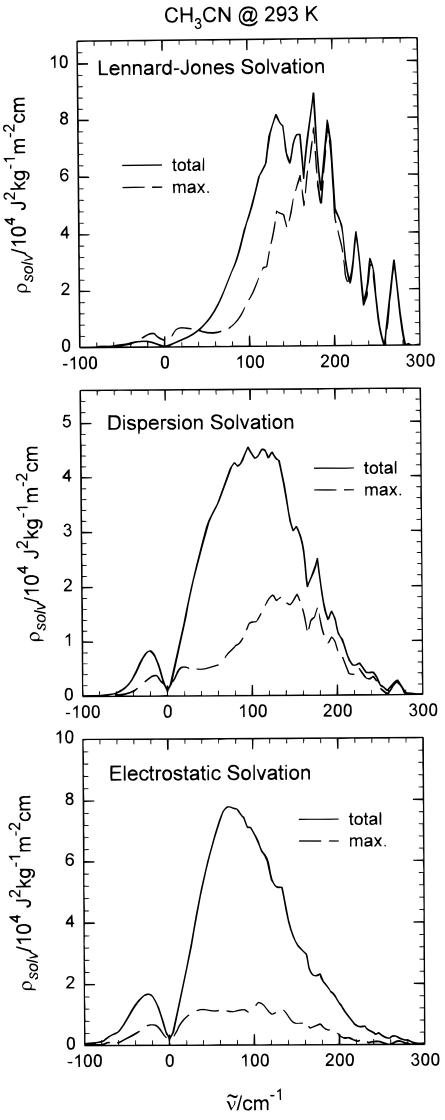

Figure 9. Solvation influence spectra for a dipolar solute dissolved in liquid CH_3CN. Each panel compares the full influence spectrum (total) with the corresponding projected spectrum in which only the motion of the solute and the single most strongly coupled solvent are included (max.). The three panels reflect three different choices of solvation probe potentials: Lennard-Jones, dispersion, and electrostatic.

dynamics that is binary drops as one goes to solvation probes less similar to vibrational friction. This preeminence of binary motion in solvation—and its subsequent dimunition with increasing range of the probe function—is graphically illustrated in Figures 8 and 9. Indeed, it does not take much beyond comparing Figure 6 with Figure 8 and comparing Figure 7 with Figure 9 to confirm that vibrational relaxation does resemble solvation dynamics and that it does so precisely to the extent to which these relaxation processes are being triggered by solute−solvent pair motions.

C. Mechanistic Studies. In view of these results on the striking spatial localization of vibrational relaxation, we really need to ask what roles the various long-range and short-range intermolecular forces at work in these liquids can be playing in the relaxation. Certainly one might have imagined that the electrostatic terms in the potential, which do, after all, contribute the vast majority of the average potential energy, would end up governing the dynamics as well. When added to the observations of vibrational population lifetimes as small as picoseconds that have been seen with ionic solutes,[7,8] and to the simulations of Whitnell, Wilson, and Hynes of the vibrational relaxation of a dipolar solute in water,[17] there would seem to be little doubt that electrostatic forces can be vital to vibrational population relaxation in polar systems.[58] A crucial role for the long-ranged forces involved in electrostatics, however, would seem to belie the very locality we are reporting here.

The resolution to this conundrum is that electrostatics are important—to determining the equilibrium liquid structure around the solute—but they are not an important ingredient in the prompt dynamics behind the relaxation in our, nonassociated, solvents. We shall defer an analysis of the equilibrium aspects of the problem to another paper,[59] but it is simple enough to subject the dynamics to a bit of mechanistic analysis. Suppose we look once again at the pieces in the INM vibrational-friction influence spectrum, but in a somewhat different fashion than we have in the past. By separating out the different contributions to the force along the vibrating bond (the A in eqs 2.1 and 2.2) we can project out the role each kind of force plays specifically in the dynamics. The immediate result (Figure 10) is that we see that the purely Lennard-Jones portion of the interaction really does account for almost all of the prompt

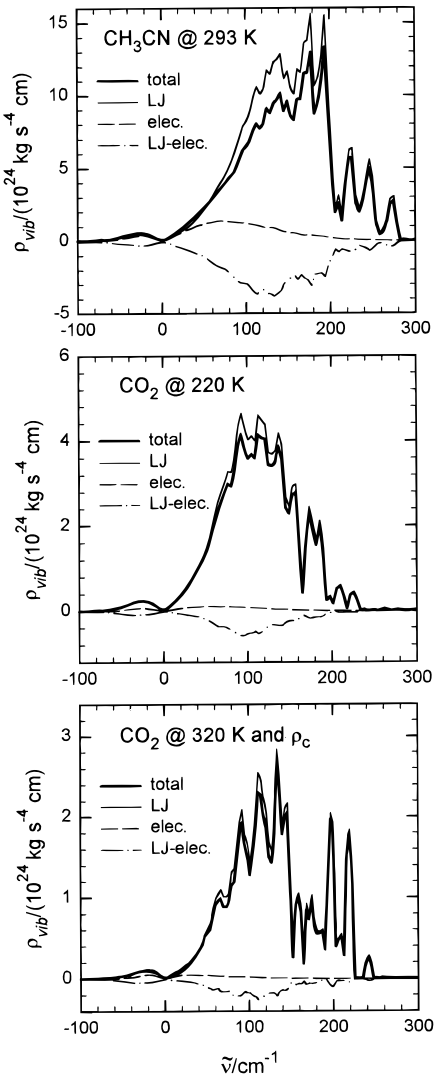

Figure 10. Contributions of different intermolecular forces to the vibrational friction influence spectrum. Each panel compares the full influence spectrum (total) with spectra in which the components arising from solely Lennard-Jones forces (LJ), solely electrostatic forces (elec.), and cross correlations between the two (LJ-elec.) have been projected out. From the top, the three panels correspond to a dipolar solute dissolved in liquid CH_3CN, I_2 dissolved in liquid CO_2, and I_2 dissolved in supercritical CO_2.

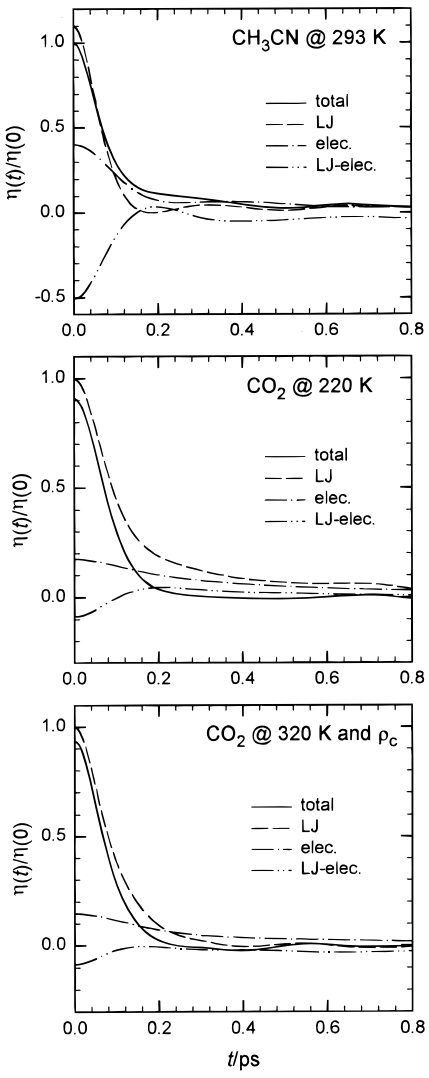

Figure 11. Contributions of different intermolecular forces to the time dependence of the vibrational friction. Each panel compares the friction derived from molecular dynamics (from the autocorrelation function of the force fluctuations felt by the rigid diatomic) with the components arising from solely Lennard-Jones forces (LJ), solely electrostatic forces (elec.), and cross correlations between the two (LJ-elec.). As with Figure 10, the three panels correspond, in descending order, to a dipolar solute dissolved in liquid CH_3CN, I_2 dissolved in liquid CO_2, and I_2 dissolved in supercritical CO_2.

dynamics, even with a dipolar solvent such as CH_3CN and a dipolar solute. Moreover, even the residual contribution that electrostatics seems to make is seen to be not so much a reflection of its direct role in the dynamics as it is an indirect effect that relies on a cross coupling to the Lennard-Jones contribution.

It is worth pointing out that we can also try to examine the time-dependent friction directly, without relying on INM theory, as has already been done in the literature[17,60] (Figure 11). A standard, and apparently quite accurate, approximation to the vibrational friction is that it is simply related to the autocorrelation function of the fluctuations of the solvent force on the rigid bond.[6,17]

$$\eta(t) = \beta\langle\delta F(0)\ \partial F(t)\rangle \tag{4.1}$$

If we decompose these force fluctuations δF into their Lennard-Jones and electrostatic pieces, then eq 4.1 tells us that the friction will automatically split into Lennard-Jones, electrostatic, and cross-correlated components.[17] A plot showing these components also seems to reveal the extent to which Lennard-Jones forces dominate the vibrational relaxation. However, what is less clear is whether one is looking at equilibrium or dynamical effects in this graph. In fact, since almost all of the distinction between Lennard Jones and electrostatic contributions seems to occur at $t = 0$, that is for $\langle(\delta F)^2\rangle$, we might have guessed the preeminence of Lennard-Jones components was largely a *static* effect.

A more illuminating approach to the elucidation of mechanisms is that detailed in section II.B, where we suggest working (at this same level of approximation) with the friction-velocity,

$$G_{FF}(t) = \langle\dot{F}(0)\ \dot{F}(t)\rangle \tag{4.2}$$

rather than the friction itself. Decomposing the exact molecular dynamics in this way in our nonpolar liquid solvent example (Figure 12) provides a number of useful lessons. For one thing, we can confirm our previous comment that the dynamics behind vibrational friction is dominated neither by center-of-mass

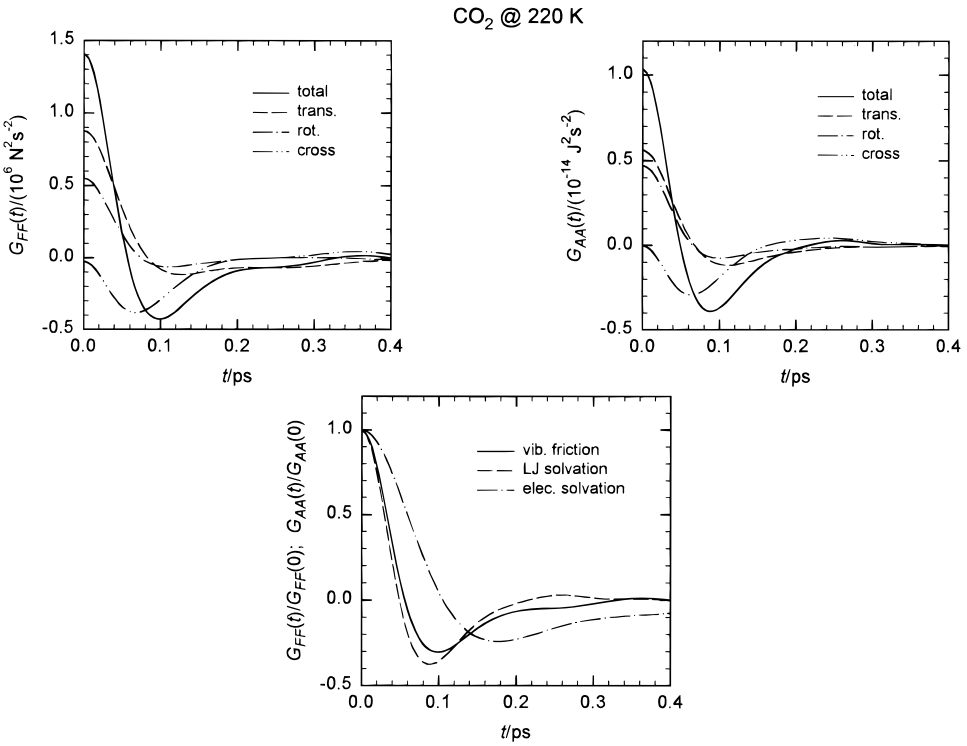

Figure 12. Relationship between the dynamics of vibrational relaxation and of solvation for an I_2 solute dissolved in liquid CO_2. The three panels show the vibrational friction-velocity correlation function (upper left), the solvation-velocity correlation function for a Lennard-Jones probe potential (upper right), and a comparison between normalized versions of the two (lower center). Each of the top two panels also shows the decomposition of the respective correlation functions (sum) into components arising from center-of-mass translation (trans.), libration (rot.), and translation−libration cross correlations (cross).

translation nor by libration. The most interesting lesson, though, stems from the comparison between Lennard-Jones solvation and vibrational friction. The quantitative similarity between the two kinds of dynamics—both in terms of the behavior of the overall time correlation functions and their individual mechanical components—makes abundantly clear the nonelectrostatic origins of the *dynamics* behind the two kinds of relaxation processes.[61] Were we to halve or double the partial charges in our intermolecular forces, as Whitnell et al. have done in their aqueous example,[17] we would no doubt find corresponding changes in the overall magnitude of the vibrational friction arising from the modifications the revised electrostatic forces induce in the equilibrium liquid structure,[59] but the dynamical mechanism, we would predict, would remain largely as it is.

As we noted in section II.B, we can also generalize the standard test for the validity of IBC theory[17,29,53,54] with the aid of this same kind of analysis. Instead of just decomposing the friction into binary and nonbinary parts, we can make a formal separation of the friction velocity, the dynamics, into binary and ternary components, Figures 13 and 14, by using eq 2.14. From the friction alone we would have been tempted to conclude that while the motion of the solute and a single solvent at a time might suffice to describe nondipolar systems such as I_2 in CO_2, for more polar situations such partitioning would no longer be useful. Yet when we extract the binary part of the friction velocity, we find that almost *all* of the dynamics for the first 0.5 ps is governed by the solute-plus-single-solvent-molecule component, even for a dipolar system. The ternary terms are certainly present in the friction, but they are evidently so slowly varying that their impact on the mechanism of vibrational relaxation is hardly felt.

All of this analysis to this point has been based on an average view of solute relaxation. The real advantage of INM approaches, however, is that they let us take an instantaneous perspective.[28] Thus the final and most critical piece of mechanistic analysis we would like to present is one that looks specifically at individual liquid configurations, Figure 15. In this figure we have returned yet again to our dipolar system and looked, as we did in Figure 7, at the influence spectra for the separate cases of vibrational friction, solvation probed by Lennard-Jones forces, and solvation probed by electrostatic forces. Without the benefit of configurational averaging, the figures seem to be an impenetrable array of random spikes, and since each spike represents the contribution of a different instantaneous normal mode, it would seem unlikely that any simple mechanistic picture would suffice to explain the data. However, a careful look at the statistics of these figures says that there is indeed a simple story to tell.

Suppose we consider first the question of how many solvent molecules are participating in the relaxation. One way to think about this problem is to note that for any given configuration, the total coupling is measured by the integral over the instantaneous influence spectrum, or equivalently, by the sum over all the modes of coupling constants squared:

$$C^2 = \int \rho_R(\omega)\, d\omega = \sum_\alpha c_\alpha{}^2 \tag{4.3}$$

But from eq 2.2 and the orthonormality of the INM eigenvectors, we know that this sum can be written as a sum of derivatives of the probe function with respect to the coordinates of each individual molecule,[22]

$$C^2 = \sum_{j=0}^{N} c_j{}^2$$

$$c_j{}^2 = \sum_\mu (m_{j\mu})^{-1} (\partial A/\partial r_{j\mu})^2 \tag{4.4}$$

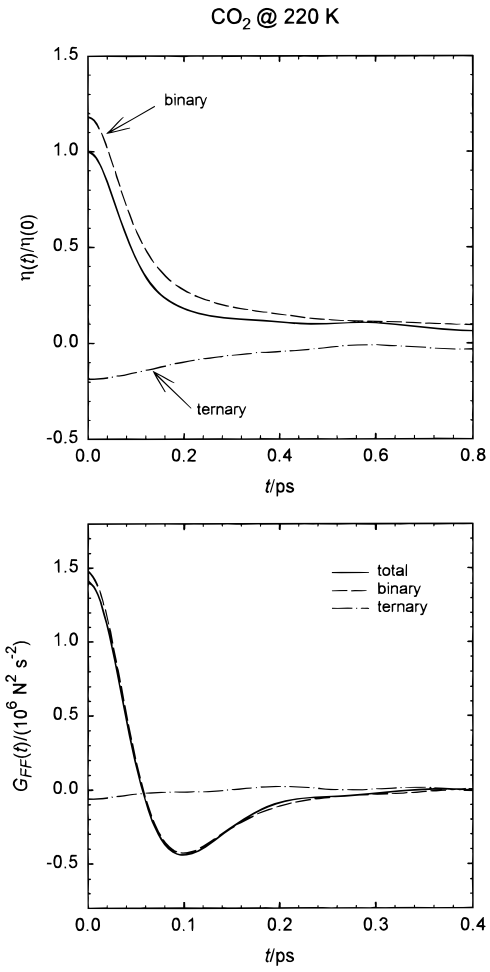

Figure 13. Contributions of simultaneous motion by two or more molecules to the vibrational relaxation of I_2 dissolved in liquid CO_2. Each panel displays a measure of the vibrational friction derived directly from molecular dynamics (as in Figure 11), along with the portions stemming from the binary (solute-plus-one-other-solvent-at-a-time) and ternary (solute-plus-two-other-solvents-at-a-time) components. The top panel exhibits the time dependence of the total friction, along with its binary/ternary decomposition, whereas the bottom panel shows the friction-velocity correlation function and its binary/ternary decomposition.

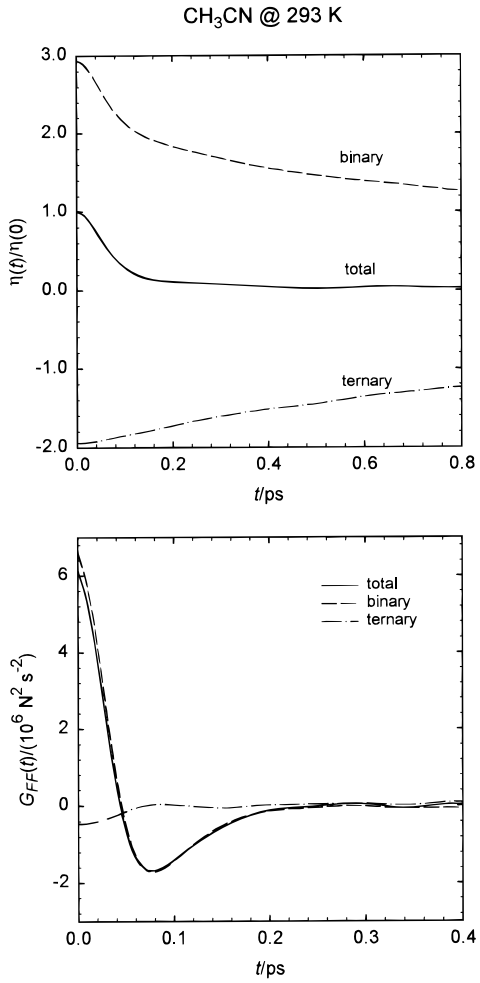

Figure 14. Contributions of simultaneous motion by two or more molecules to the vibrational relaxation of a dipolar solute dissolved in liquid CH_3CN. As with Figure 13, the two panels show the solute-plus-single-solvent (binary) and solute-plus-two-solvents (ternary) components of the time-domain friction and of the friction-velocity correlation function, both obtained directly from molecular dynamics.

with $m_{j\mu}$ the mass appropriate to each coordinate μ of molecule j. So what we would really like to know is how many of the N solvent molecules it typically takes to comprise a significant fraction of this total coupling sum. A selection of eight different liquid configurations with $N = 107$ shows that anywhere from as few as four to as many as 17 different solvent molecules can contribute at the 1% level. The *median* number of contributing molecules though—the average number of solvent molecules it takes to recover 50% of the total coupling—is far more informative. As we can see from Table 3, vibrational population relaxation and Lennard-Jones solvation are quite similar mechanistically in that they are both typically triggered by the motion of a single solvent. Dispersive solvation usually takes closer to three and electrostatic solvation on the order of five solvent molecules, but even these numbers are remarkably low considering that in these systems the first solvation shell alone contains about 15 solvents.[22,23]

Given that at most a few molecules are playing the key roles in the solute relaxation from any one liquid configuration, the next question to ask is just what motions these molecules are undergoing. Here is where the complexities of the remainder of the liquid enter the picture, for the INM answer to the question is that these critical molecules are performing whatever motions the multitude of modes they are involved in tell them to, and each individual mode can be quite collective. Still there is a certain amount of simplicity awaiting us even here. Our study of atomic solvents revealed that regardless of what most of a mode's dynamics entailed, the net effect of the active modes was merely to modulate the distance between the solute and a key solvent or two.[28] We were therefore able to encapsulate most of the high-frequency aspects of the relaxation in terms of a single two-molecule effective harmonic mode for each configuration. It seems not unreasonable to expect that a similar scenario will govern relaxation in molecular fluids.

But, even in advance of any such study for our molecular system, we can point to yet another noteworthy simplification. Figure 15 makes it appear that a sizeable (and highly variable number) of instantaneous normal modes are contributing to the instantaneous relaxation. But, suppose we look (Table 3) at the median number of contributing modes, defined (by analogy with the median number of contributing solvents) to be the average number required to achieve 50% of the total coupling in eq 4.3. What we find is that only a "mesoscopic" number of modes really contribute. That is, instead of seeing participation from some macroscopic fraction of the 540 modes present in our 108 molecule system (or some microscopic number corresponding to the 1−5 key solvents), we find intermediate

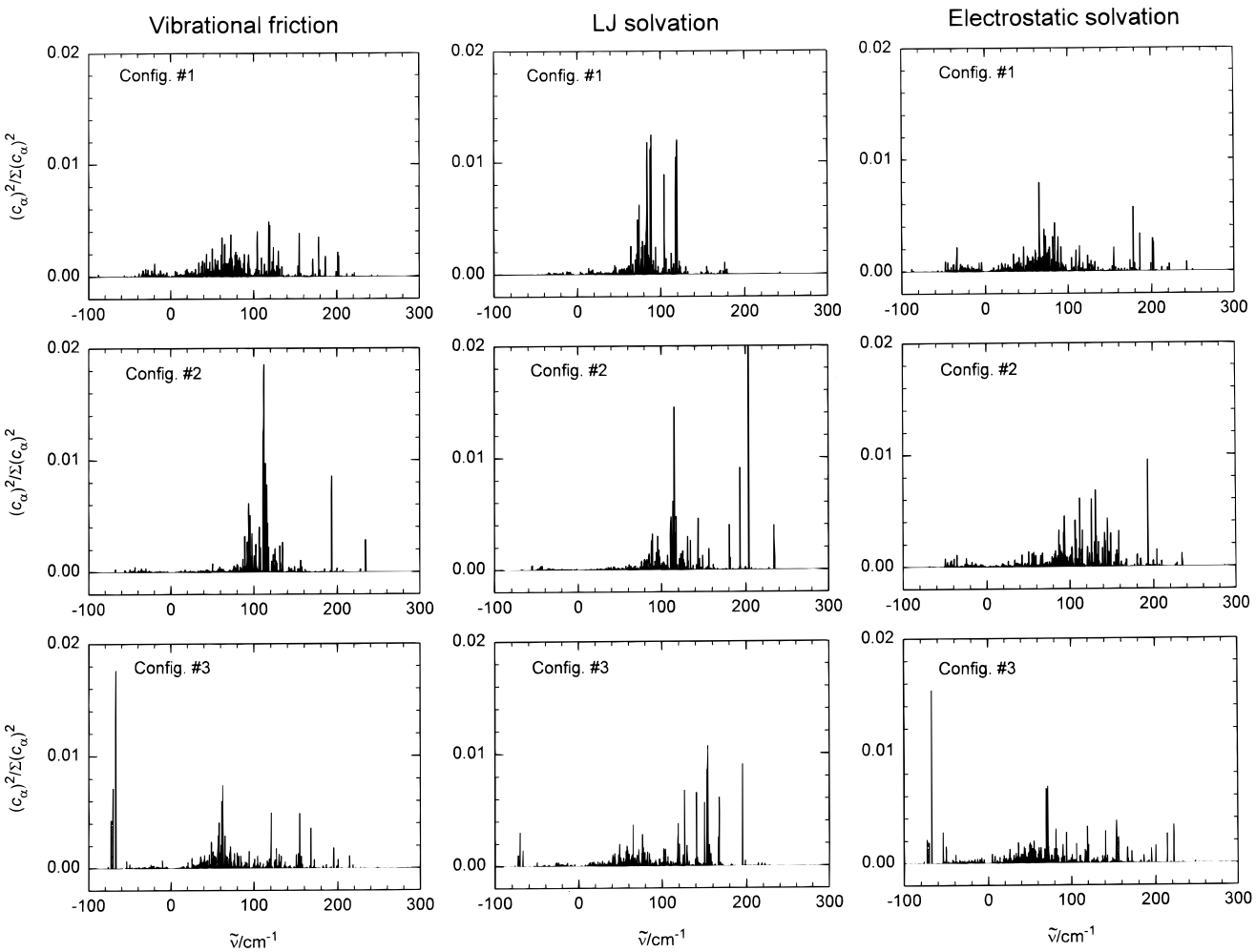

Figure 15. Instantaneous influence spectra for a dipolar solute dissolved in liquid CH_3CN. Each of the three rows shows, for a distinct liquid configuration, three different normalized distributions of instantaneous-normal-mode coupling strengths $(c_\alpha)^2$ for modes α at the indicated frequencies. The three columns, from left to right, distinguish the instantaneous vibrational friction spectrum, the instantaneous solvation spectrum arising from a Lennard-Jones probe potential, and the instantaneous solvation spectrum arising from an electrostatic probe potential. For visual clarity, the coupling strengths are portrayed by spikes with zero width.

TABLE 3: Instantaneous Contributions to Solute Relaxation[a]

	vibrational relaxation	solvation[b]		
		LJ	dispersive	electrostatic
number of solvents	1.38	1.50	2.75	4.63
number of modes[c]	19.8	15.1	23.4	33.0

[a] Median numbers of solvents and median numbers of instantaneous normal modes contributing to the relaxation taking place in a given liquid configuration. All data shown are derived from a simulation of liquid CH_3CN involving 107 solvent molecules and a single diatomic solute. The results reported here are averaged over eight configurations separated in time by 16 ps. [b] Solvation dynamics as probed by Lennard Jones (LJ), dispersion forces (dispersive), or electrostatic interactions (electrostatic). [c] By way of comparison, there are 540 total modes in these systems. Note that the square root of this number of modes is 23.2.

values, on the order of $(540)^{1/2}$.[62] Though this kind of result is strongly reminiscent of some sort of fluctuation phenomenon, its exact origins are unclear. It should prove interesting to learn just how the solute selects out its special modes.

V. Concluding Remarks

Since we have now been able to perform the same level of short-time analysis of vibrational population relaxation in molecular liquids that we had undertaken for solvation dynamics in the same liquids, we should certainly be asking ourselves what broad, general insights we might have gained into how solute relaxation occurs. Without question, our principal finding is that the mechanism governing relaxation in these systems depends far more on the features of the dynamics being probed ("the spectroscopic probe function") than on the character of the solvent. In particular, in this paper we looked not only at the probe appropriate to vibrational relaxation (the force on a vibrating bond), but at probes germane to solvation (the Lennard-Jones, dispersive, and electrostatic parts of the solute-solvent potentials), and we did so in both dipolar and nondipolar solvents and in both sub- and supercritical solvents. The end result was clear: it was the probe that was mechanism determining.

The basic mechanism of vibrational population relaxation, it seems, is almost identical to that seen in Lennard-Jones probes of solvation. The large fraction of the prompt dynamics controlled by the joint motion of the solute and a single solvent and the nearly statistical fraction driven by center-of-mass translation rather than libration are remarkably similar with these two probes and quite distinct from that seen with longer range solvation probes. When we proceed to the single-liquid-configuration level, we find the similarity extends there as well: the median numbers of contributing solvents and con-

tributing instantaneous normal modes show much the same parallelism between the two short-ranged probes. Even the precise shapes of the average influence spectra for these two kinds of experiments serve to emphasize this striking connection. The fact that the influence spectra are so similar for the short-ranged probes points out that precisely the same modes of the solution—with precisely the same special weightings—are being called upon to carry out the relaxation. Conversely, as the probe becomes longer and longer ranged, it is apparent that a rather different set of weightings comes into play. By the time we turn to electrostatic probes, the underlying modes are contributing far more equally, making the influence spectrum closer to the basic density of states of the liquid itself.

Of course, of equal note to this pronounced dependence on the specific probe is the lack of dependence of vibrational relaxation mechanisms on the specific solvent. Regardless of the system, all of our work shows a distinctly binary flavor to the onset of vibrational relaxation. From a macroscopic perspective, the isolated-binary-collision-like scaling of relaxation rates with local density has long been appreciated,[53] but we can now supplement that with more microscopic statements: It is evidently just the prompt dynamics that is limited to the solute and a single solvent; at longer times a more collective behavior does take over. Yet, at the short times that control vibrational relaxation, it is equally clear that it takes the motions of typically no more than one or two nearby solvent molecules to trigger vibrational relaxation, even with a dipolar solvent. Consistent with this observation, it is the shortest range parts of the intermolecular interaction—the Lennard-Jones terms in the standard representations of the potential—that end up governing the relaxation, even with a dipolar solvent. While Whitnell et al. seemed to find otherwise in their study of vibrational relaxation in water,[17] it could very well be that their example was a rather special case. In looking at vibrational relaxation in the vicinity of 650 cm^{-1} they were focusing on relaxation caused entirely by coupling to water's hydrogen-bond dominated librational modes.[63] Since both the water structure around their solute and their model of hydrogen bonding are strongly intertwined with the electrostatic forces, their result is perhaps not as opposed to ours as it might seem.[58]

Our efforts, it should be pointed out, have in some ways been quite limited. By concentrating only on solutes with a single internal vibrational mode, and on rigid models for our solvents, we have limited our energy transfer studies to V-T and V-R processes. We have therefore excluded the interesting possibilities that can arise when the solvent can assist in intramolecular vibrational relaxation[14−16] or can facilitate relaxation by absorbing the solute's vibrational energy into its own internal vibrations.[14,16] Just what the mechanisms are behind these more involved processes (which are so crucial to vibrational relaxation of any molecule larger than a diatomic) we look forward to learning. However, it is worth noting that with the aid of the findings in this paper we have now learned enough to overcome one of the other limitations of this work, that of the inability of a (linearized) instantaneous-normal-mode theory to accomodate solute vibrations with frequencies higher than those encompassed in the solvent's own density of states.[26] The central role of binary motions, it turns out, tells us how to include the necessary anharmonic effects into our analysis. We shall use this insight in a subsequent paper to describe high-frequency vibrational relaxation.[64]

Acknowledgment. Though we were unable to include this paper in the recent special issue of this Journal dedicated to Daniel Kivelson, it is a pleasure to dedicate this paper to him. His insights into relaxation processes in liquids and his general approach to physical chemistry have greatly benefited the field as a whole and us in particular. We are delighted, as well, to thank Grant Goodyear, Ross Larsen, and Edwin David for insightful comments on the application of instantaneous normal modes to solute relaxation. We also thank Bruce Berne and Tom Keyes for several quite helpful discussions. This work was supported by NSF grants to B.M.L. (CHE-9520619) and to R.M.S. (CHE-9417546 and CHE-9625498). B.M.L. also acknowledges the Donors of the Petroleum Research Fund as administered by the American Chemical Society.

TABLE 4: Fits to Simulated Vibrational Frictions[a]

	$\eta(0)^b$	A_1	A_2	α_1/ps^{-2}	α_2/ps^{-1}	b^c
CO_2, 220 K[d]	0.617	0.627	0.208	51.2	1.56	22.9
CO_2, 320 K, ρ_c[e]	0.331	0.525	0.108	105	5.35	24.3
CO_2, 320 K, 2.5ρ_c[e]	1.20	0.734	0.194	76.3	1.03	28.2
CH_3CN, 293 K[f]	1.51	0.709	0.125	136	2.30	33.3

[a] The parameters used to fit the vibrational friction computed from molecular dynamics to the form described in the Appendix. [b] The static friction in units of kg s^{-2}. [c] In units of radians ps^{-1}. [d] I_2 dissolved in liquid CO_2. [e] I_2 dissolved in supercritical CO_2. The notation ρ_c refers to the critical density. [f] Dipolar "Br_2" dissolved in liquid CH_3CN.

Appendix

To perform numerical Fourier transforms of the vibrational friction we compute from molecular dynamics, we find it useful to fit the friction to an analytical function. In this Appendix we describe this fit.

We represent the friction normalized to its zero time value with the expression

$$\eta(t)/\eta(0) = \exp(-\alpha_1 t^2)\left[A_1 + A_2\cos(bt) + \frac{1-A_1-A_2}{b}\sin(bt)\right] + (1-A_1-A_2)\exp(-\alpha_2 t)$$

This functional form satisfies the requirement that $\dot{\eta}(0) = 0$, it has the correct long-time behavior, and it seems to provide an excellent fit for our systems. We attribute no particular physical significance to the five parameters, though.

With this form it is a simple matter to take the cosine transform, enabling us to write $\eta_R(\omega)$, the real part of the frequency domain friction, from eq 2.8.

$$\eta_R(\omega) = \eta(0)\left\{\frac{A_1}{2}\sqrt{\frac{\pi}{\alpha_1}}\exp\left(-\frac{\omega^2}{4\alpha_1}\right) + \frac{A_2}{4}\sqrt{\frac{\pi}{\alpha_1}}\left[\exp\left(-\frac{(b-\omega^2)}{4\alpha_1}\right) + \exp\left(-\frac{(b+\omega)^2}{4\alpha_1}\right)\right] + (1-A_1-A_2)\frac{\alpha_2}{2b\sqrt{\alpha_1}}\left[D\left(\frac{b-\omega}{2\sqrt{\alpha_1}}\right) + D\left(\frac{b+\omega}{2\sqrt{\alpha_1}}\right)\right] + (1-A_1-A_2)\frac{\alpha_2}{\alpha_2^2+\omega^2}\right\}$$

where $D(x)$ is Dawson's integral,

$$D(x) = \exp(-x^2)\int_0^x \exp(t^2)\,dt$$

a special function that can be found in most numerical algorithms packages.

The parameters we found for this form for our systems are reported in Table 4.

References and Notes

(1) Gordon, R. G. Adv. *Mag. Res.* **1968**, *3, 1.*

(2) Tokmakoff, A.; Fayer, M. D. *Acc. Chem. Res.* **1995**, *28*, 437.

(3) Zimdars, D.; Tokmakoff, A.; Chen, S.; Greenfield, S. R.; Fayer, M. D.; Smith, T. I.; Schwettman, H. A. *Phys. Rev. Lett.* **1993**, *70*, 2718. Tokmakoff, A.; Zimdars, D.; Sauter, B.; Francis, R. S.; Kwok, A. S.; Fayer, M. D. *J. Chem. Phys.* **1994**, *101*, 1741.

(4) Vanden Bout, D.; Berg, M. J. *Raman Spectrosc.* **1995**, *26*, 503.

(5) Vanden Bout, D.; Muller, L. J.; Berg, M. *Phys. Rev. Lett.* **1991**, *67*, 3700. Muller, L. J.; Vanden Bout, D.; Berg, M. *J. Chem. Phys.* **1993**, *99*, 810. Ianaba, R.; Tominaga, K.; Tasumi, M.; Nelson, K. A.; Yoshihara, K. *Chem. Phys. Lett.* **1993**, *211*, 183. Vanden Bout, D.; Freitas, J. E.; Berg, M. *Chem. Phys. Lett.* **1994**, *229*, 87.

(6) Tuckerman, M.; Berne, B. J. *J. Chem. Phys.* **1993**, *98*, 7301.

(7) Owrutsky, J. J.; Raftery, D.; Hochstrasser, R. M. *Annul Rev. Phys. Chem.* **1994**, *45*, 519.

(8) Li, M.; Owrutsky, J. J.; Sarisky, M.; Culver, J. P.; Yodh, A.; Hochstrasser, R. M. *J. Chem. Phys.* **1993**, *98*, 5499.

(9) Heilweil, E. J.; Casassa, M. P.; Cavanagh, R. R.; Stephenson, J. C. *Annu. Rev. Phys. Chem.* **1990**, *40*, 143.

(10) Tokmakoff, A.; Sauter, B.; Fayer, M. D. *J. Chem. Phys.* **1994**, *100*, 9035.

(11) Chen, S.; Hong, X.; Hill, J. R.; Dlott, D. D. *J. Phys. Chem.* **1995**, *99*, 4525. Hong, X., Chen, S. Dlott, D. D. *J. Phys. Chem.* **1995**, *99*, 9102.

(12) Graener, H.; Seifert, G.; Laubereau, A. *Chem. Phys. Lett.* **1990**, *172*, 435.

(13) Tokmakoff, A.; Fayer, M. D. *J. Chem. Phys.* **1995**, *103*, 2810.

(14) Ambroseo, J. R.; Hochstrasser, R. M. *J. Chem. Phys.* **1988**, *89*, 5956.

(15) Tokmakoff, A.; Sauter, B.; Kwok, A. S.; Fayer, M. D. *Chem. Phys. Lett.* **1994**, *221*, 412.

(16) Moore, P.; Tokmakoff, A.; Keyes, T.; Fayer, M. D. *J. Chem. Phys.* **1995**, *103*, 3325. Rey, R.; Hynes, J. T. *J. Chem. Phys.* **1996**, *104*, 2356.

(17) Whitnell, R. M.; Wilson, K. R.; Hynes, J. T. *J. Phys. Chem.* **1990**, *94*, 8625. Whitnell, R. M.; Wilson, K. R.; Hynes, J. T. *J. Chem. Phys.* **1992**, *96*, 5354.

(18) Stratt, R. M. *Acc. Chem. Res.* **1995**, *28*, 201.

(19) Keyes, T. J. *Phys. Chem.* **1997**, *A101*, 2921.

(20) It is not necessarily possible to perform a rigorous resolution of an arbitrary motion of the solvent into a *linear* combination of INMs. The INM density of states does have only a finite bandwidth. Nonetheless this resolution can often be accomplished approximately, as illustrated by linear INM solvation theory and by the INM theory of vibrational population relaxation, for example. One can also systematically enlarge the available bandwidth by coupling to INMs at higher powers than linear. Larsen, R. E.; Stratt, R. M. In preparation. The present paper will be concerned with dynamics at the linear level.

(21) Stratt, R. M.; Cho, M. *J. Chem. Phys.* **1994**, *100*, 6700.

(22) Ladanyi, B. M.; Stratt, R. M. *J. Phys. Chem.* **1995,** *99*, 2502.

(23) Ladanyi, B. M.; Stratt, R. M. *J. Phys. Chem.* **1996**, *100*, 1266.

(24) Goodyear, G.; Larsen, R. E.; Stratt, R. M. *Phys. Rev. Lett.* **1996**, *76*, 243.

(25) Goodyear, G.; Stratt, R. M. *J. Chem. Phys.* **1996**, *105*, 10050.

(26) Goodyear, G.; Stratt, R. M. *J. Chem. Phys.* **1997**, *107*, in press.

(27) Kindt, J. T.; Schmuttenmaer, C. *J. Chem. Phys.* **1997**, *106*, 4389. Keyes, T. *J. Chem. Phys.* **1996**, *104*, 9349. Ladanyi, B. M.; Klein, S. *J. Chem. Phys.* **1996**, *105*, 1552.

(28) Larsen, R. E.; David, E. F.; Goodyear, G.; Stratt, R. M. *J. Chem. Phys.* **1997**, *107*, 524.

(29) Oxtoby, D. W. *Adv. Chem. Phys.* **1981**, *47* (part 2), 487. Chesnoy, J.; Gale, G. M. *Adv. Chem. Phys.* **1988**, *70* (part 2), 297. Harris, C. B.; Smith, D. E.; Russell, D. J. *Chem. Rev.* **1990**, *90*, 481.

(30) Binary behavior has also been successfully invoked in an instantaneous-normal-mode study of solvation in high-pressure gases. See: Kalbfleisch, T. S.; Ziegler, L. D.; Keyes, T. *J. Chem. Phys.* **1996**, *105*, 7034.

(31) Pure dephasing is discussed in the context of generalized-Langevin-equation and harmonic-bath representations of vibrational relaxation by: Levine, A. M.; Shapiro, M.; Pollak, E. *J. Chem. Phys.* **1988**, *88*, 1959. Georgievskii, Yu. I.; Stuchebrukhov, A. A. *J. Chem. Phys.* **1990**, *93*, 6699. Tuckerman, M.; Berne, B. J. Ref 6.

(32) Landau, L.; Teller, E. *Z. Sowjetunion* **1936**, *10*, 34.

(33) We shall not be concerned in this paper with quantum mechanical aspects of vibrational relaxation beyond those automatically included in the Fourier transform of the classical friction. For a clear discussion of this issue see: Bader, J. S.; Berne, B. J. *J. Chem. Phys.* **1994**, *100*, 8359.

(34) Stratt, R. M.; Maroncelli, M. J. *Phys. Chem.* **1996**, *100*, 12981.

(35) An alternative approach to predicting frequency-dependent vibrational friction using INM theory is explored in: Schvaneveldt, S. J.; Loring, R. F. *J. Chem. Phys.* **1995**, *102*, 2326. Schvaneveldt, S. J.; Loring, R. F. *J. Chem. Phys.* **1996**, *104*, 4736. Schvaneveldt, S. J.; Loring, R. F. *J. Phys. Chem.* **1996**, *100*, 10355. For the approach described in this paper, we employ the notation that a (nonboldface) subscript R denotes the cosine transform (the *real* part of the Fourier−Laplace transform), whereas a boldface subscript **R** refers to a result obtained for a single liquid configuration. We also note that eq 2.9 is valid only for $\omega \neq 0$, since we have omitted a formal contribution from an additional term proportional to $\delta(\omega)$.

(36) Buchner, M.; Ladanyi, B. M.; Stratt, R. M. *J. Chem. Phys.* **1992**, *97*, 8522.

(37) Steele, W. A. *Mol. Phys.* **1987**, *61*, 1031.

(38) Allen, M. P.; Tildesley, D. J. *Computer Simulation of Liquids*; Clarendon Press: Oxford, 1987.

(39) Edwards, D. M. F.; Madden, P. A.; McDonald, I. R. *Mol. Phys.* **1984**, *51*, 1141.

(40) Murthy, C. S.; O'Shea, S. F.; McDonald, I. R. *Mol. Phys.* **1983**, *50*, 531.

(41) Stone, A. J.; Alderton, M. *Mol. Phys.* **1985**, *56*, 1047.

(42) Rappé, A. K.; Casewit, C. J.; Colwell, K. S.; Goddard, W. A., III; Skiff, W. M. *J. Am. Chem. Soc.* **1992**, *114*, 7864.

(43) Stace, A. J.; Murrell, J. N. *Mol. Phys.* **1977**, *22*, 1.

(44) Kennedy, J. T.; Thodos, G. *J. Chem. Eng. Data* **1960**, *5*, 293.

(45) The triple-point temperature of CO_2 is 216.5 K and the corresponding liquid density is 1.18 g/cm. See ref 44.

(46) The critical temperature of CO_2 is 304 K. See ref 44.

(47) Some recent theoretical work characterizing vibrational relaxation in atomic solvents in some detail is that of ref 6 and the following: Berne, B. J.; Tuckerman, M. E.; Straub, J. E.; Bug, A. L. R. *J. Chem. Phys.* **1990**, *93*, 5084. Egorov, S. A.; Skinner, J. L. *J. Chem. Phys.* **1996**, *105*, 7047.

(48) INM theory can be shown to encompass even solute vibrational frequencies outside the basic IBM band when nonlinear coupling is included. See ref 20.

(49) Gnanakaran, S.; Hochstrasser, R. M. *J. Chem. Phys.* **1996**, *105*, 3486. Gnanakaran, S.; Lim, M.; Pugliano, N.; Volk, M.; Hochstrasser, R. M. *J. Phys. Condens. Matter* **1996**, *8*, 9201.

(50) This, most efficient solvent, *j*, is defined to be the one that leads to the maximum value of the square coupling constant c_j^2 in eq 4.4.

(51) For these systems, with relatively heavy solutes, the solute contributions are modest, as one might have expected by analogy with the discussion in ref 23. However, it is worth noting that the solute does contribute 12.5% of the vibrational friction spectrum in the CH_3CN example. In view of the discussion in section IV.B, this figure might be compared with the analogous results for solvation in CH_3CN. The percentage solute contributions to the solvation influence spectrum with Lennard Jones, dispersion, and electrostatic probe potentials are 14.6%, 5.7%, and 4.5%, respectively.

(52) That is, the solvent molecule for which there is the shortest solute-site/solvent-site distance is deemed to be the closest solvent.

(53) Davis, P. K.; Oppenheim, I. *J. Chem. Phys.* **1972**, *57*, 505. Oxtoby. D. *Mol. Phys.* **1977**, *34*, 987. Chesnoy, J. Weis, J. J. *J. Chem. Phys.* **1986**, *84*, 5378. Paige, M. E.; Harris. C. B. *Chem. Phys.* **1990**, *149*, 37. Paige, M. E.; Harris. C. B. *J. Chem. Phys.* **1990**, *93*, 3712. Russell, D. J.; Harris, C. B. *Chem. Phys.* **1994**, *183*, 325.

(54) Fixman, M. *J. Chem. Phys.* **1961**, *34*, 369. Zwanzig, R. *J. Chem. Phys.* **1961**, *34*, 1931. Zwanzig, R. *J. Chem. Phys.* **1962**, *36*, 2227. Dardi, P. S.; Cukier, R. I. *J. Chem. Phys.* **1988**, *89*, 4145. Dardi, P. S.; Cukier, R. I. *J. Chem. Phys.* **1991**, 95, 98.

(55) Maroncelli, M. *J. Mol. Liq.* **1993**, *57*, *1*.

(56) Yu, J.; Kang, T. J.; Berg, M. *J. Chem. Phys.* **1991**, *94*, 5787. Fourkas, J. T.; Berg, M. *J. Chem. Phys.* **1993**, *98*, 7773. Fourkas, J. T.; Benigno, A.; Berg, M. *J. Chem. Phys.* **1993**, *99*, 8552. Ma. J.; Vanden Bout, D.; Berg, M. *J. Chem. Phys.* **1995**, *103*, 9146.

(57) An interesting complementary exploration of precisely the same kinds of distinctions is provided by: Stephens, M. D.; Saven, J. G.; Skinner, J. L. *J. Chem. Phys.* **1997**, *106*, 2129.

(58) The suggestion has been made that while electrostatic forces can be quantitatively important, their effects may not always be as dramatic as that seen in ref 17. See: Benjamin, I.; Whitnell, R. M. *Chem. Phys. Lett.* **1993**, *204*, 45.

(59) Ladanyi, B. M.; Stratt, R. M. *J. Mol. Liq.*, in preparation.

(60) See, for example, ref 58 and the following: Ferrario, M.; Klein, M. L. McDonald, I. R. *Chem. Phys. Lett.* **1993**, *213*, 537.

(61) The analogous calculation for a dipolar solute in CH_3CN reveals much the same kinds of mechanistic and time-scale similarities between Lennard-Jones-mediated solvation and vibrational relaxation, but somewhat less similarity in the depths of the minima of the corresponding $G(t)$ functions.

(62) A similar square-root-like dependence was observed for the number of "participating" modes when we carried out a finite-size-scaling study for vibrational relaxation in atomic fluids. See ref 26 (footnote 85).

(63) Cho, M.; Fleming, G. R.; Saito, S.; Ohmine, I.; Stratt, R. M. *J. Chem. Phys.* **1994**, *100*, 6672.

(64) Larsen, R. E.; Stratt, R. M. In preparation.